smaller T. The scatter of the circles and triangles in Fig. 1 for $Ka_0>7$ comes from the fact that Khare and Moiseiwitsch[4] gave their cross sections for large K only to three significant figures. Note that the zero in Fig. 4 is displaced.

Recently, Vriens *et al.*[8] measured differential cross sections for 2^3S excitation of helium and found large discrepancies between experimental and Ochkur (theory) cross sections. Miller and Krauss[26] thereupon calculated differential Born-Oppenheimer and Ochkur 2^3S cross sections, and found these two approximations to be in excellent agreement above 100 eV.

Since the Ochkur approximation is a good approximation to the Born-Oppenheimer approximation for such entirely different processes as elastic scattering and 2^3S excitation, the same may be true for other transitions. The experiment of Vriens *et al.*,[8] however, casts serious doubt upon the validity of exchange approximations in which only first-order terms are included, for electron energies of a few hundred eV. One must keep in mind, however, the possibility that these exchange approximations may become valid at much higher electron energies, since it is known that cross sections for 2^1S excitation in helium are only in good agreement with the Born approximation for electron energies above about 1500 eV.

[26] K. J. Miller and M. Krauss, J. Chem. Phys. (to be published).

ACKNOWLEDGMENTS

The authors are grateful to G. E. Chamberlain for valuable discussions on this subject, to Y. K. Kim and M. Inokuti for the permission to use their elastic Born scattering amplitudes prior to publication, and to S. P. Khare for sending them the results of Ref. 4 in tabular form. The authors further wish to thank J. W. Cooper and U. Fano for valuable comments. One of us (L. V.) wishes to thank J. Arol Simpson and K. G. Kessler for enabling him to work as a guest worker in the Atomic Physics Division.

PHYSICAL REVIEW VOLUME 170, NUMBER 1 5 JUNE 1968

Detachment of Electrons from H^- and O^- Negative Ions by Electron Impact*

G. C. Tisone† and L. M. Branscomb
Joint Institute for Laboratory Astrophysics,‡ Boulder, Colorado 80302
(Received 4 December 1967)

The energy range for the electron detachment cross section for H^- has been extended down to 8.4 eV. The absolute cross section for detachment of electrons from atomic-oxygen negative ions has been measured in the energy range 7.1 to 487.1 eV. Results of these measurements are compared with Bethe-Born calculations of the cross section. This calculation with the semiclassical Coulomb correction is in qualitative agreement with the experimental results above 20-eV electron energy for both H^- and O^-, although the energy dependence of the H^- cross section from 100 to 500 eV is not consistent with the slope predicted theoretically for the high-energy limit.

I. INTRODUCTION

THE cross section for detachment of electrons of the negative hydrogen ion by electron impact has been the subject of a large number of theoretical predictions,[1–5] with discordant results, and two experiments.[6,7] The Bethe-Born (BB) approximation as used by McDowell and Williamson[2] with the semiclassical Coulomb repulsion of Geltman[1] was found to be in best agreement with our experiment.[6] This previous measurement for H^- did not extend to low enough energies to ascertain the validity of the Coulomb correction. The energy range of the H^- cross section has been extended in the work reported here down to 8.4 eV, where a comparison of the experiment and the BB calculation with the Coulomb correction can be made. Since the cross section for electron detachment from negative ions may be expected to depend strongly on electron affinity and the negative-ion structure, we have also made a study of the detachment of electrons

* This work was supported in part by the Advanced Projects Research Agency (Project DEFENDER) under Contract No. DA-31-124-ARO-D-139, monitored by the U. S. Army Research Office (Durham), and by the Office of Naval Research under Order No. NA-onr-2-64, Contract No. NR 012-111.

† Present address: Sandia Laboratory, Albuquerque, N. M.

‡ Of the University of Colorado and the National Bureau of Standards.

[1] S. Geltman, Proc. Phys. Soc. (London) **75**, 67 (1960).

[2] M. R. C. McDowell and J. H. Williamson, Phys. Letters **4**, 159 (1963).

[3] M. R. H. Rudge, Proc. Phys. Soc. (London) **83**, 1 (1964).

[4] B. M. Smirnov and M. I. Chibisov, Zh. Eksperim. i Teor. Fiz. **49**, 841 (1965) [English transl.: Soviet Phys.—JETP **22**, 585 (1966)].

[5] M. Rogalski, Acta Phys. Polon. **29**, 15 (1966).

[6] G. Tisone and L. M. Branscomb, Phys. Rev. Letters **17**, 236 (1966).

[7] D. F. Dance, M. F. A. Harrison, and R. D. Rundel, Proc. Roy. Soc. (London) **A299**, 525 (1967), referred to as DHR.

from O^- (whose binding energy is 1.46 eV, compared to 0.75 eV for H^-) by electron impact, using the BB approximation as a basis for comparison of theory with experiment.

The cross section for detachment by electrons was studied using modulated crossed-beam techniques. This valuable technique has been employed previously in the study of processes such as photodetachment and electron collisions with neutral particles. Until 1961 crossed-beam technique had not been used to study processes where both beams are charged. Dolder, Harrison, and Thonemann[8] made the first such cross-section measurement. They investigated the ionization of He^+ by electrons, and later also measured the ionization cross sections for Ne^+ and N^+.[9] Wareing and Dolder have measured[10] the ionization cross section for Li^+, which is isoelectronic with H^-. Recently the ionization cross sections of alkali atomic ions have been measured by Lineberger *et al.*[11] and Hooper *et al.*[12] Also, Dunn and Van Zyl[13] have measured the cross section for dissociation of H_2^+ by electron impact. In addition, studies of excitation of ions have been made by this method.[14] The referenced papers contain discussions of the particular pitfalls of crossed-beam experiments in which both particles in the initial state are charged. In our work an additional difficulty is imposed by the fact that the final particle to be detected is neutral.

In a successful crossed-charged-beam experiment which purports to determine an absolute cross section, it is necessary that the signal-to-noise ratio be sufficient, and also that the "signal" be unambiguously identified with the physical process which the investigator claims to be studying. This requires a model or theory for the experiment, which includes all physical phenomena which may plausibly contribute to the signal. One must then demonstrate that one can distinguish experimentally between the various possible sources of signal to which the detector can respond, isolating the phenomenon intended for study. The experimental arrangement, and especially the "labeling" of the incident beams by periodic modulation, is designed to minimize the number and difficulty of the tests which must be made to make that unambiguous identification.

In spite of these difficulties, there is an important advantage of the crossed-beam technique for charged particles over the usual neutral gas target when collisions of charged and neutral particles are studied. Cross sections for interaction of two charged beams can be determined in terms of currents or particle fluxes and a geometrical form factor that can be measured directly. In addition, all charged particles can be unambiguously identified by their momenta and energies. The rate of formation of neutral particles at the intersection of two time-varying, collimated beams (at 90°) by the process

$$X^-+e\rightarrow\sum_{n,l}X_{n,l}{}^0+2e, \tag{1}$$

whose cross section is σ (cm^2), is given by

$$N_0(t)=\sigma\frac{(v^2+V^2)^{1/2}}{vV}\frac{1}{e^2}\int i(z,t)j(z,t)dz, \tag{2}$$

where $i(z,t)$ and $j(z,t)$ are, respectively, the current densities per centimeter of the ion and electron currents in the z direction at time t. Measurement of these current densities will be discussed later. The z direction is perpendicular to the plane containing the ion and electron beams. The beams are assumed to vary slowly in time, in relation to the ratio of each beam's thickness to the other's velocity. The spatial and time variations can then be separately integrated. The electron and ion velocities are, respectively, v and V; e is the electronic charge.

In the experiment reported in this paper, a collimated beam of mass-analyzed H^- or O^- ions, at 2.5-keV energy, is bombarded in high vacuum by a collimated beam of electrons of controlled energy between 7 and 500 eV. The resulting neutral H or O atoms are detected, and the cross section is computed from Eq. (2) after other sources of signal are shown to have been eliminated.

If the ion and electron beams did not individually produce appreciable currents in the neutral detector, a direct-current experiment could be performed as described by Eq. (2). However, the cross section for stripping of electrons off of negative ions in collisions with gas molecules is known to be of the order of 10^{-15} cm^2 at a few keV.[15] Thus for a gas density N, path length L, and current I, one expects stripped neutrals to be created at a rate given by

$$N_0(\text{strip})=(I/e)(\sigma_s LN+C), \tag{3}$$

where the constant C accounts for the possibility of ions being converted to neutrals on slit edges and other surfaces. To illustrate the importance of stripping, we can simplify Eq. (2) by taking the integral over the two current distributions as equal to $eI\times10^{15}$, which refers to 0.3-mA electron current in our geometry. I is the total ion current. We take the velocity factor as 10^{-7} sec/cm. Thus, putting $N=3\times10^{16}p$ (p in Torr),

[8] K. T. Dolder, M. F. A. Harrison, and P. C. Thonemann, Proc. Roy. Soc. (London) **A264**, 367 (1961).
[9] K. T. Dolder, M. F. A. Harrison, and P. C. Thonemann, Proc. Roy. Soc. (London) **A274**, 546 (1963); Proc. Phys. Soc. (London) **82**, 368 (1963).
[10] J. B. Wareing and K. T. Dolder, Proc. Phys. Soc. (London) **91**, 887 (1967).
[11] W. C. Lineberger, J. W. Hooper, and E. W. McDaniel, Phys. Rev. **141**, 151 (1966).
[12] J. W. Hooper, W. C. Lineberger, and E. W. McDaniel, Phys. Rev. **141**, 165 (1966).
[13] G. H. Dunn and B. Van Zyl, Phys. Rev. **154**, 40 (1967).
[14] D. F. Dance, M. F. A. Harrison, and A. C. H. Smith, Proc. Roy. Soc. (London) **A290**, 74 (1966).
[15] S. K. Allison, Rev. Mod. Phys. **30**, 1137 (1958).

and taking $\sigma=30\pi a_0^2$ and $L=20$ cm, we have

$$\frac{N_0(\text{strip})}{N_0}\sim\frac{600p+C}{3\times10^{-7}}. \quad (4)$$

Thus, even at a pressure of 3×10^{-8} Torr, which is a typical operating pressure for this experiment, gas stripping produces 60 times as many neutrals as electron bombardment.

Another possible source of current in the neutral detector can be derived from the electron gun, for a significant number of soft x rays are produced by the electrons when they strike metal parts in the gun. In practice we find this signal to be two orders of magnitude smaller than that from stripped neutrals, and thus comparable to the desired signal. All such signals, which are proportional to the current of one of the two beams, but not to their product, may be distinguished from neutrals which are proportional to the product of electron and ion currents by modulating both beams at different frequencies and detecting the mixed signal. Of course, this does not eliminate all influence of the stripped background on the experiment; shot noise from this background still produces the dominant source of noise in the experiment.

II. THEORY OF MODULATION AND ac DETECTION

If we assume that the electron and ion beams are chopped to produce symmetric, periodic, rectangular-wave currents at repetition frequencies ω_j and ω_i, respectively, the current densities at any given instant of time can be written

$$j(z,t)=\bar{j}(z)+(4/\pi)\bar{j}(z)(\sin\omega_j t+\tfrac{1}{3}\sin3\omega_j t+\cdots) \quad (5)$$

and

$$i(z,t)=\bar{i}(z)+(4/\pi)\bar{i}(z)(\sin\omega_i t+\tfrac{1}{3}\sin3\omega_i t+\cdots). \quad (6)$$

Here, $\bar{i}(z)$ and $\bar{j}(z)$ are time averages. It is not necessary that the beams be chopped symmetrically, but it is convenient to have this condition so that only the average dc currents need to be measured. The time-dependent neutral signal, with the first harmonics, reaching the neutral detector can be found by substituting Eqs. (5) and (6) in Eq. (2):

$$N_0(t)=\frac{4\sigma(v^2+V^2)^{1/2}}{\pi e^2vV}\int\bar{i}(z)\bar{j}(z)dz[\sin\omega_j t+\sin\omega_i t+\frac{4}{\pi}(\sin\omega_j t\sin\omega_i t)+\frac{4}{3\pi}(\sin\omega_i t\sin3\omega_j t+\sin\omega_j\sin3\omega_i t)+\cdots]. \quad (7)$$

It is convenient to define the form factor F,

$$F=\frac{\int\bar{i}(z)\bar{j}(z)dz}{\int\bar{i}(z)dz\int\bar{j}(z)dz}=(IJ)^{-1}\int\bar{i}(z)\bar{j}(z)dz, \quad (8)$$

which has dimensions of L^{-1} and in this experiment was typically 4 cm^{-1}. I and J are the total, time-averaged ion and electron currents. Then we can write

$$N_0(t)=N_0(\text{peak})[\sin\omega_j t+\sin\omega_i t+(4/\pi)(\sin\omega_j t\sin\omega_i t)+(4/3\pi)(\sin\omega_i t\sin3\omega_j t+\sin\omega_j t\sin3\omega_j t)+\cdots], \quad (9)$$

where

$$N_0(\text{peak})=\frac{4\sigma(v^2+V^2)^{1/2}}{\pi e^2vV}JIF. \quad (10)$$

One method of detecting the double modulation signal, i.e., the part of the signal proportional to the product I times J, would be to detect the signal at the sum or difference frequency that results from the second term or from the higher harmonics; this method uses only one of the sidebands. Another method was used in this experiment. Our modulation and detection scheme makes use of both of the sidebands and is shown in Fig. 1. With this method, the electron modulation frequency (20 kHz) is made large compared to the ion-beam modulation frequency (50 Hz). (The high modulation frequency for the electrons is also a necessary condition to eliminate pressure modulation by the electrons, as discussed below.) Two lock-in amplifiers are used in series, with the electron modulation frequency ω_j being synchronized to the first lock-in amplifier and the ion-beam modulation frequency ω_i being synchronized to the second. The electron modulation frequency must be large compared to the ion modulation frequency so that the high frequency and both of its sidebands will be in the pass band of the first amplifier. The output time constant of the first amplifier is kept short compared to the low-frequency period.

Included in the signal arriving at the first amplifier will be background signals due to both electrons (via photons) and stripping of ions on residual gas in the chamber. The neutral detector converts a neutral flux N_0 into a voltage S_0. We can define the neutral detector gain G_d as the constant of proportionality between S_0

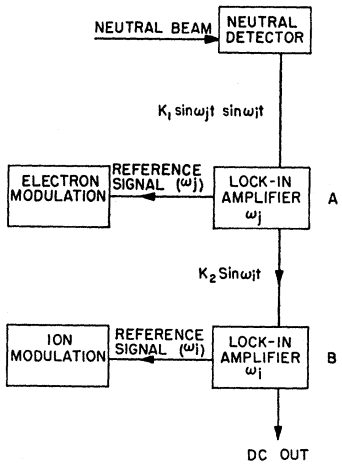

FIG. 1. Detection of the double-modulated signal using two lock-in amplifiers in series.

and N_0. The total signal at the input to the first lock-in will then be given by

$$S_0=N_0(\text{peak})G_d\left\{\left[\frac{4}{\pi}\sin\omega_j t\sin\omega_i t+\frac{4}{3\pi}(\sin\omega_i t\sin 3\omega_j t+\sin\omega_j t\sin 3\omega_i t)\right]+\cdots\right\}+G_dA_j\sin\omega_j t+G_dA_i\sin\omega_i t, \quad (11)$$

where A_j and A_i are the amplitudes from the first two terms in Eq. (9) and from the background signals due to the modulated ion and electron currents individually. If the gain of the first lock-in is G_1, the signal out of the first lock-in is

$$S_1=\frac{1}{\tau_1}\int_t^{\tau_1+t} G_1G_d\sin(\omega_j t+\psi_j)\times\left[\frac{4}{\pi}N_0(\text{peak})\sin\omega_i t\sin\omega_j t+A_j\sin\omega_j t+\cdots\right]dt. \quad (12)$$

Here, τ_1 is the time constant of the output circuit and is set so that terms in the frequency ω_j are averaged out. The phase ψ_j is adjustable.

We ensure that $\tau_1\ll 1/\omega_i$, so that the phase shift due the integration of Eq. (12) is small. Thus, the second lock-in receives a signal

$$S_2=(4/\pi)N_0(\text{peak})G_1G_d\cos\psi_j\sin\omega_i t+G_1A_J\cos\psi_j. \quad (13)$$

The output of the second amplifier is then given by

$$S_3=\frac{1}{\tau_2}\int_t^{\tau_2+t}2G_1G_2G_d\frac{4}{\pi}N_0(\text{peak})\cos\psi_j\sin\omega_i t(\omega_i t+\psi_i)dt=\frac{4}{\pi}G_1G_2G_dN_0(\text{peak})\cos\psi_i\cos\psi_j, \quad (14)$$

where $\tau_2\gg 1/\omega_i$. The signal is maximized by making ψ_i and ψ_j equal to $n\pi$. The signal out is then given by

$$S_3=\frac{4}{\pi}G_1G_2G_dN_0(\text{peak})=\frac{4^2}{\pi^2}G_1G_2G_d\frac{\sigma(v^2+V^2)^{1/2}}{e^2vV}IFJ. \quad (15)$$

The method of calibration of the neutral detector measures the product $(4^2/\pi^2)G_1G_dG_2$.

This same detection scheme was used for a different method of beam chopping where the electrons and the ion beam were chopped at the same frequency (about 5000 Hz). The electrons were then switched in and out of phase with the ions at 50 Hz. About one-half the O^- data were taken with this arrangement, and no systematic differences in the resulting cross section were found.

III. SOURCES OF UNWANTED SIGNAL

We have shown above how the double modulation scheme reduces the problem of background signals from ion and electron beams into a noise-level problem, since these individual signals will average to zero in sufficient time. A more serious problem arises if any phenomenon in the experiment can mix signals proportional to electron and ion currents other than the process [Eq. (1)] under study. We will define as "spurious" or unwanted any signal not averaging to zero with increasing time detected by the lock-ins and not resulting from the ionization of the negative ions. We will discuss the problem of spurious signals now, so that the description of the details of the experimental design can be understood in the light of the need to minimize spurious signal sources.

Possible sources of such signals include the following:

(1) A modulated (at ω_j) attenuation of the negative-ion beam if the gas pressure in the collision region is modulated by the electron beam. At low enough frequencies the electron beam can cause a periodic outgassing of the electron collector, resulting in a double-modulated stripped beam.

(2) When double modulation is used, there is a possibility that the currents of stripped neutrals at ω_i will exceed the dynamic range over which the detector and its associated electronics are accurately linear, thus resulting in electronic mixing of the two background single-frequency signals.

(3) The modulated negative-ion beam can be deflected, periodically, by the space charge of the electron beam in the collision region. This can produce a cross modulation in the detected stripped neutral signal if either the number of stripped particles reaching the detector is affected, or if the detector is slightly sensitive to the point of impact of the neutrals.

The ideal test for unwanted signals is to search for them at electron energies below the threshold for the reaction under study. Although successfully used by Dolder, Lineberger, and other workers for other processes, this method is not available to us because the threshold for ionization of H^- lies at only 0.75 eV.

A. Pressure Modulation

The modulation of the pressure due to the outgassing of the surface collecting the electrons can be eliminated by choosing a sufficiently high modulation frequency for the electrons. If the rate of out-gassing of metal surfaces struck by the electron beam modulated at frequency ω is given by $W=W_0\sin\omega t+W_1$, where W_1 includes the steady component of out-gassing due to elevated temperatures in the gun, the pumping speed from the electron gun is S, and its volume is V, we find for the gas density N/V in the gun

$$N/V=W_0[S^2+\omega^2V^2]^{-1/2}\sin(\omega t+\delta)-W_1/S.$$

To ensure that the alternating component of the background is small, it is necessary to ensure that the amplitude of the sine function be small. Although the pumping speed out of the electron gun may be only some ten liters per second, the product ωV is about 10^3 liters per sec at 20 kHz. Data taken at a lower frequency (5 kHz) produced cross-section values not significantly different, in comparison with statistical uncertainties. The importance of effects such as this can be shown by noting that the desired signal is usually 1 to 10 times less than stripped background from the collision region even at 5×10^{-8} Torr. Thus, a 10% modulation in the total pressure in the electron gun at the electron modulation frequency is necessary to produce a signal the same magnitude as the desired signal.

B. Nonlinear Mixing of Background Signals

One test for nonlinearities in the detection system is to determine whether the signal is linearly proportional to I and J. Such a test is essential to show that the signal has the functional dependence shown in Eq. (2). However, since the background currents at the detector exceed the wanted signal by two orders of magnitude, the most sensitive test for nonlinear mixing is made by varying the background current levels. This is done by deliberately increasing the pressure in the background vacuum, and thus increasing the gas stripping of the ions.

C. Space-Charge Modulation of the Stripped Neutrals

The stripped neutral current can become modulated at the electron beam chopping frequency if two conditions are fulfilled: (a) The electron beam space charge is sufficient to change the spatial distribution of the negative ions passing through it, and (b) these small changes in trajectory are detected through nonuniformities in the sensitivity of the neutral detector. Such a nonuniformity can be caused either by changes in sensitivity across the detector surface or possibly by a small fraction of the ions which, having suffered a scattering slightly out of the beam, are caused to fall just inside or outside the detector aperture.

These trajectory changes will necessarily be very slight under our conditions. The maximum potential in the electron beam is estimated at substantially less than 1 V; a 2500-eV beam just to one side of a 1-cm ribbon of this beam will be deflected of the order of 10^{-4} rad. In fact, great care is taken to see that the electron and ion beams are coplanar, as shown by the form-factor measurements. Nonetheless, the space-charge modulation can be observed when one artificially raises the background pressure or misaligns the beam so that it passes near one edge of the entrance aperture to the neutral detector.

If the neutrals which transmit the space-charge modulation are formed in gas collisions, a study of the pressure dependence of the signal will reveal their presence, and the data can be extrapolated to zero pressure. On the other hand, if the neutrals are formed in a collision with a metal wall, the effect will be pressure-independent. Its absence must be demonstrated by a study of the beam path and the effect on the total signal of altering this path with electric fields. It is important to note that the only slits or walls that can cause this effect are those which are placed *after* the ion beam has passed through the electron beam. The exit aperture to the collision region is sufficiently large that the only plausible surfaces of concern are the plates used to sweep ions out of the neutral beam and the Faraday cup which collects them. A necessary but not sufficient condition that the effect is negligible is the demonstration that the neutral signal is independent of trajectories in the region after the collision volume.

We now proceed to a discussion of the details of the experimental apparatus, at the end of which (Sec. IV F) we will present examples of the data used to satisfy ourselves that the sources of spurious signal are under adequate control.

IV. GENERAL DESCRIPTION OF THE BEAM APPARATUS

A. Beam Optics and Vacuum System

A schematic diagram of the experiment is shown in Fig. 2. Details of the ion source, the electron gun, and the neutral detector are described later. Ions from the hot cathode source are extracted and focused by the lens system before entering the 90° mass spectrometer. The beam is chopped by a set of deflecting plates shown just before the mass spectrometer. When entering the mass spectrometer, the ion beam must be approximately parallel, in order to produce a focus at the exit slit. After passing through the mass spectrometer, the ions are refocused by a lens system to produce a parallel beam which enters the collision region. The ion beam is deflected 5° before entering the collision region. This deflection eliminates neutral particles formed before the collision region by gas stripping, particularly in the previous section of the vacuum system where background pressures were up to 100 times higher. The deflectors are located as near to the electron gun as is physically possible. After passing through the electron gun, the negative ions are deflected into a collecting cup. The electron and ion beam profiles in the collision region are determined by a scanning plate which permits a determination of the form factor F. Negative-ion beams were of the order of 4×10^{-8} A.

The beam apparatus has three stages of differential pumping. The first stage of pumping, which is after the ion source, utilizes a mercury diffusion pump. Typical pressures in this stage are usually 5×10^{-5} Torr when the ion source is running. The second stage and

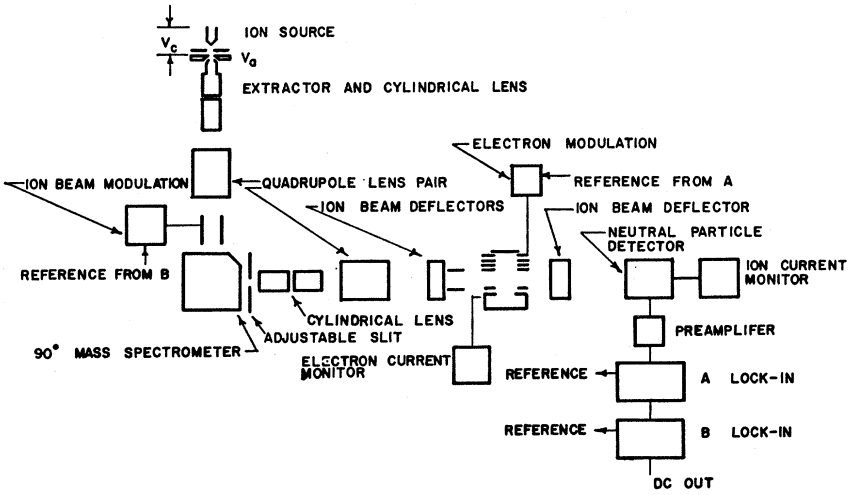

FIG. 2. Schematic diagram of the experiment.

collision region both utilize ion pumps. The usual base pressure in the collision region is 2×10^{-8} Torr, which with ion source and electron gun operating rises to 5×10^{-8} Torr.

B. Electron-Gun Design

The final version of the electron gun used in this experiment is shown in Fig. 3, and is similar to that shown in a paper by Simpson and Kuyatt.[16] This design was used after it was found that a well-defined, parallel beam could not be obtained by using a simple triode which consisted of the cathode, a screen for a grid, and the collision box for the anode.

The electron-gun design utilized a flat oxide cathode about 2.54 cm long. It was intended that the width of the electron beam be defined by the aperture at the entrance to the collision region. The design for the first three elements of the lens system were described by Soa, and further studied by Simpson and Kuyatt.[16] Data for this type of lens system, with circular apertures, are given in the paper by Simpson and Kuyatt.

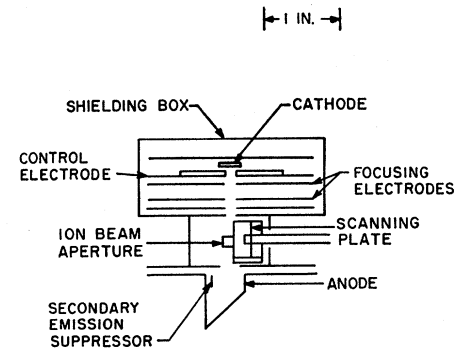

FIG. 3. Diagram of the electron gun showing the slit lens system, the electron collector, and the position of the electron- and ion-beam scanning plate.

[16] J. A. Simpson and C. E. Kuyatt, Rev. Sci. Instr. 34, 265 (1963).

The electron beam enters the collision region as a ribbon, 1.27 mm high and 25.4 mm long. At the higher energies its divergence is small and it passes through the center of the ion beam. At the lowest energies (10 eV) the electron beam diverges up to a factor of 2 in width at the plane of the ion beam, so that its width is comparable to that of the ion beam, which is accurately rectangular and of 2.8 mm width.

The electron beam was modulated by applying a negative-going rectangular wave of about 50 V to the control electrode of the electron gun. This ac voltage was clamped to the control-electrode bias voltage. The frequency of modulation, 20 kHz, was chosen for two reasons. First, the frequency has to be high enough that no detectable modulation of the pressure is produced by the electron beam. Second, the frequency must be large compared to the beam modulation frequency, as required for the double-modulation method of detection.

The scanning plate, shown in Fig. 4, is used to determine the spatial distribution of the electron current and ion beams. This plate was used instead of the usual scanning slits because of limited space in the collision region. Although this method is not as convenient as having a slit to get differential current dis-

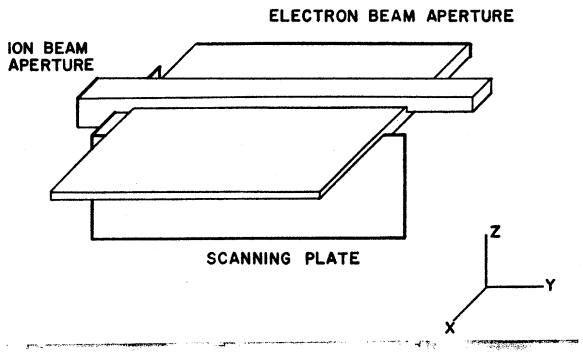

FIG. 4. Operation of the scanning plate. The plate is shown intersecting both of the beams.

tributions directly, the same information is contained in the integral curves that are obtained with the scanning plate. The travel of this scanning plate is calibrated in terms of the micrometer screw used to drive the plate mechanism. The departures from linearity in the travel of this plate are less than 1% over the whole range.

A retarding energy analysis of the electron beam using the anode as a repeller has demonstrated that the electron beam has an energy spread of 1.0 to 1.5 V. The energy of the electrons is 3.0 ± 0.5 V lower than the voltage at the cathode, and this correction is applied to the cathode voltage to determine the effective electron energy. The error allowance is assumed large enough to account for any difference in contact potential between the collision region and anode, which are all constructed of Advance alloy. A calculation of the maximum space-charge potential in the center of the electron beam for the highest currents and lowest energies used gives shifts of less than 0.1 eV. The input impedance of the circuit that measures the electron current was kept low (200 Ω) to minimize the transverse field across the ion beam generated by the potential of the electron collector. The maximum potential, at $J=3\times10^{-4}$ A, is 0.06 V, which is almost entirely shielded from the ion beam by the grounded collision box. These calculations also encourage us to believe that the maximum angular deflection of the 2.5-keV ion beam by the space charge will be very small compared to the neutral deflector aperture.

Another correction to the energy scale is required to express the result in center-of-mass energies: If E represents the electron kinetic energy and W the ion energy, then for 90° relative angle

$$E_{\text{c.m.}}=\frac{M}{m+M}\left(E_{\text{lab}}+W_{\text{lab}}\frac{m}{M}\right).$$

Therefore, approximating $M/(m+M)=1$, and knowing that the ions have 2.5-keV laboratory energy, we must add to the electron laboratory energy 1.4 eV for H^-, 0.7 eV for D^-, and 0.09 eV for O^-.

In order to ensure that the measured electron current is accurately the electron current which passed through the ion beam, a plate is located on one side of the anode (see Fig. 3) and provides a transverse field which suppresses secondary emission. At every electron energy, the collected current was measured as a function of this suppressing field. The data were taken when the collection was saturated and independent of small changes in the suppressor voltage. A further advantage to the study of the cross section with different transverse fields in the electron collector for suppressing electrons has been noted by Harrison.[17] The attendant defocusing of the electrons when they finally strike the electron collector reduces the modulated out-gassing of the collector, particularly for high electron energies.

[17] M. F. A. Harrison (private communication).

C. Neutral-Particle Detector

The final product in this experiment is a neutral particle. Various methods to detect neutral particles are available, but many do not meet the requirements of this experiment, which are listed below.

(1) The particle detector should have high enough sensitivity to detect the final flux of atoms of about 10^4 sec^{-1}.

(2) The detector sensitivity should not change when the vacuum system is opened to air and subsequently pumped down again.

(3) We must ensure that small deflections of the background stripped neutral beam, caused by modulated space charge in the collision region, do not produce an ac signal in the neutral detector larger than 10^{-4} of the stripped current, and thus contribute more than 1% to the desired signal. The neutral detector must, therefore, have an aperture free of grids or Venetian-blind dynodes and safely larger than the outer edges of the beam. A circular aperture of 10-mm diameter proved adequate. A further requirement is that the detector must have an effectively uniform response across its surface.

(4) Since large numbers of hard photons were originally expected, it was desirable that the device be relatively insensitive to photons or have the possibility of discriminating against photons.

The final design for the neutral-particle detector, shown in Fig. 4, is similar to that used by Daly[18] for detecting positive particles. The detector consists of a copper-beryllium plate with surface at an angle of 30° to the beam and a plastic scintillator[19] (NE102) in front of a photomultiplier tube. The secondary emitting plate is biased at a high negative voltage (~10 to 15 kV) and the secondary electrons are accelerated into the plastic scintillator. The scintillator is coated with a thin film of aluminum having a depth of 500 Å, so that the surface of the plastic will not charge. This film also reflects the light being produced in the scintillator, thus improving its efficiency.

The secondary plate was placed in a cup with a 10-mm-diam aperture. This cup produced focusing of the electrons onto the scintillator surface. All of the high-voltage components were then placed in a grounded shield as shown in Fig. 5. The aperture to this shield has a slow-ion collecting plate to shield the detector from slow positive ions.

Secondary emission is also increased by having the incident beam strike the plate at a small angle. Chambers[20] has found that about two electrons per incident H^0 atom could be expected from Cu-Be at 2.5 keV and small angles of incidence. Chambers also found that the number of secondaries per incident H^+

[18] N. R. Daly, Rev. Sci. Instr. 31, 264 (1960).
[19] Nuclear Enterprises, Ltd., Winnepeg, Canada.
[20] E. S. Chambers, Phys. Rev. 133, A1202 (1964).

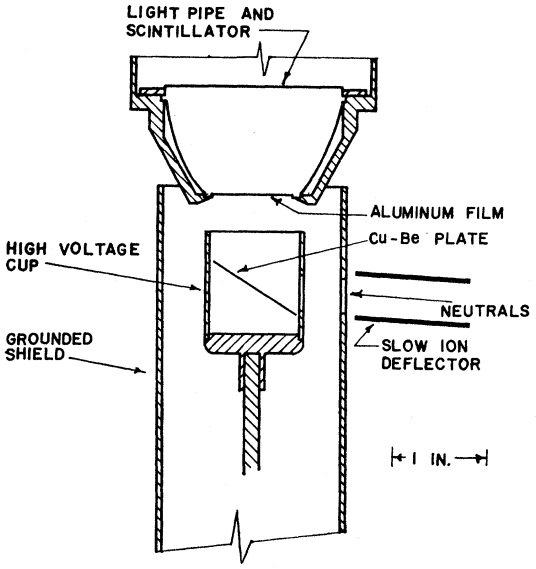

FIG. 5. Operation of the neutral-particle detector. Neutral atoms striking the Cu-Be plate produce 2.0 to 2.6 electrons per particle. These electrons are then accelerated into the plastic scintillator.

ion was about equal to that for the H^0 atom. Our detector yields an average of 2.6 electrons for neutral hydrogen and 2.0 electrons for neutral oxygen with 2.5-keV energy. Precise agreement with Chambers's result should not be expected since no effort was made to match his experimental conditions. The stability of the secondary-emission coefficient γ for our gas-covered surface is more important than the absolute value of γ, since our detector is independently calibrated.

The photons produced near the surface of the scintillator are transferred to the photomultiplier tube by an exponential light pipe as shown in Fig. 5. The light pipe and scintillator have been constructed from one piece of scintillator material. With this design all the photons hitting the sides are internally reflected, and their loss results primarily from absorption. The vacuum seal is made directly between the light pipe and the stainless-steel housing with epoxy resin.

The secondary plate was usually run with a bias of 10 to 15 kV. The threshold of operation was found at a bias of 2.5 kV. Above this energy the number of photons slowly increased with the energy of the secondary electrons. The bias of 10 kV was a compromise between maximizing the gain of the detector and minimizing voltage breakdowns.

D. Calibration of the Neutral Detector

If the secondary-electron emission coefficient for the neutrals, $\gamma(X^0)$, is known, the neutral-particle detector and its associated electronics can be calibrated by using the neutrals formed by stripping on the background gas. When neutral particles are impinging upon the plate shown in Fig. 5, the current leaving the detector cup and plate is a measure of the neutral-particle flux if $\gamma(X^0)$ is known. A double-modulated neutral beam is obtained by electrically chopping the negative-ion beam at both the high and low frequencies using a special circuit built for this purpose. A neutral signal from stripping which is identical in wave form to the signal from the electron-detachment experiment is obtained. After measuring the average neutral flux, the detector and its associated electronics can be turned on and calibrated. The quantity $\gamma(X^0)$ was measured in a separate photodetachment experiment where a known number of neutrals was produced. $\gamma(X^0)$ was compared to $\gamma(X^-)$, which could be measured during each electron-detachment experiment to make sure that the sensitivity of the detector did not change.

Chambers[20] found the number of secondary electrons per neutral hydrogen atom at 2.5 keV to be about 10% higher than that for protons. From this one can expect that the secondary emission coefficient for the negative ions should be similar to that for neutral atoms. The secondary-emission coefficient for the neutrals was measured in a separate photodetachment experiment. In the photodetachment process,

$$h\nu + X^- \rightarrow X + e, \tag{16}$$

the ejected electron current is numerically equal to the neutral "current." A measure of these electrons defines a neutral beam flux I^0, thus permitting a measurement of $\gamma(X^0)$ in the detector. For comparison, the secondary-emission coefficient for negative ions was measured at the same time.

The arrangement for this photodetachment experiment is shown in Fig. 6. A beam of white light (about 40 W) intersected the ion beam at about the center of the capacitor. The beam deflection shown in Fig. 6 is the same as that used when the electron gun is in place. Beyond the reaction region the ion beam is deflected into the collector and the neutral particles continue

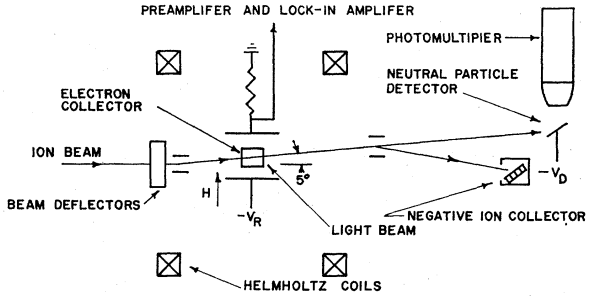

FIG. 6. Schematic diagram of the photodetachment experiment for the comparison of the secondary electron coefficients of the negative ion and the neutral atoms. The number of electrons collected in the photodetachment region is a measure of the number of neutrals hitting the Cu-Be plate.

into the detector plate just as in the ionization experiment. A negative voltage was applied to the lower plate of the capacitor (repeller) and the electrons were collected on the opposite plate. A magnetic field of 50–100 G, which is shown in Fig. 6, was used to assist in the collection of the electrons. [Tests were made to ensure that the neutral detector gain was not appreciably affected by (a) the magnetic field, or (b) the 1° deflection of the incoming H^- ion beam caused by the repeller voltage.]

The voltage that is applied to the repeller must be large enough so that all electrons from the photodetachment process are collected; saturation curves show this to be true at an operating field of 12 V/cm in the capacitor. The value of $\gamma(X^0)$ is then found by measuring the secondary electron current I^+ (a positive current for a meter connected to the plate and cup), leaving the Cu-Be plate when this plate and cup is biased at -75 V:

$$\gamma(X^0)=I^+/eI^0.$$

The secondary-emission coefficient $\gamma(X^-)$ was obtained for negative ions as follows: The negative-ion beam was allowed to fall on the copper-beryllium plate, and its current I^- was measured by biasing the plate and cup at a positive voltage (+75 V) and measuring the current to the cup. Reflection of the negative ions and production of secondary ions at the surface should not be important in this measurement. Available literature on the interaction of ions with surfaces[21] indicates that contributions due to these effects should be less than 3%. The plate and cup was then biased at a negative voltage (−75 V), and the difference between the number of electrons leaving and the number of negative ions arriving, I^+, was measured. The secondary-electron coefficient is then given by

$$\gamma=I^+/I^-+1. \tag{17}$$

The currents measured at the detector cup were saturated at ±75 V and were of the order of 10^{-8} to 10^{-7} A. This measurement of $\gamma(X^-)$ was made in identical fashion during the photodetachment measurement of $\gamma(X^0)$ and on the occasion of every measurement of the ionization cross section. The ratio of the secondary-emission coefficients of neutral H to H^- was found to be 1.0±0.09, and for O to O^- was found to be 1.0±0.12.

When the Cu-Be plate was first installed, the measured secondary-electron coefficient was found to be 3.00 for H^- ions and 2.28 for D^- ions. After a period of two months, which included opening of the vacuum system several times, these coefficients deteriorated to about 2.6 for H^- ions and 2.0 for D^- ions. The secondary emission coefficients then stabilized at these latter values for the duration of the experiment (several months). The vacuum system was opened to air several times during this period. The equilibrium γ for O^- was found to be about 2.0.

The calibration procedure during each detachment experiment first requires a measurement of $\gamma(X^-)$ as described above, from which $\gamma(X^0)$ is found from the ratio $\gamma(X^-)/\gamma(X^0)$ given in the photodetachment experiment. The cup is biased at a negative voltage, and only stripped neutal atoms allowed to enter the detector. The average current leaving the cup is measured:

$$I^+=\gamma(X^0)eN(X^0). \tag{18}$$

The average number of neutrals $N(X^0)$ is then computed from Eq. (18). The ion beam from which these neutrals are derived is double modulated to give it a wave form capable of detection by the ac circuitry used for the signal in the experiment. Thus, ac detection of this neutral beam completes the calibration procedure.

The oxygen atoms produced by photodetachment will be predominately in the ground state, while up to one-third of the neutral atoms formed by electron-impact ionization can be expected to be in the ^1D metastable state.[22] This is not expected to change the calibration of the neutral detector since this metastable state is only 2 V above the ground state, and provides potential energy which is small compared to the 2.5-keV kinetic energy. It should also be noted that slow metastable $He(2^3S)$ atoms with an excitation energy of 20 eV produce[23] a maximum 0.25 electrons per atom. This value is only 12% of the secondary-electron-emission coefficient for the $O(^3P)$ atom.

E. Collection of Data

A total integration time of 75 to 150 sec was usually necessary to reduce random fluctuations of single measurements to 2 to 10%. This length of integration time allowed diagnostic tests such as pressure dependences and current dependence to be done in a reasonable length of time. Pressure dependences were taken at all electron energies. Signals with small pressure dependences could then be corrected to zero pressure. Current dependences were taken at selected points, and the signal was always found to be linear with the respective current. Drift in the gain of the neutral detector and the associated electronics was tested for by repeating the data at an electron energy of 100 eV.

The integrals of the current distributions, $\int_0^z i(z')dz'$ and $\int_0^z j(z')dz'$, were measured for each of the different electron energies. The current distributions $i(z)$ and $j(z)$ were then calculated by numerical differentiation and the resulting numbers were used to calculate the form factor F. Values of F varied from 4.0 to 2.8 cm^{-1} over the electron energy range.

The data presented in this paper were taken over a period of 16 months under many different conditions

[21] See the review by M. Kaminisk, *Atomic and Ionic Impact on Metal Surfaces* (Academic Press Inc., New York, 1965), pp. 248, 249.

[22] L. M. Branscomb, S. J. Smith, and G. Tisone, J. Chem. Phys. **43**, 1 (1965).

[23] J. B. Hasted, J. Appl. Phys. **30**, 22 (1959).

TABLE I. H^- detachment cross section.

Electron energy (eV)	Cross section (πa_0^2)	Limit of systematic error in relative cross section[a] (%)
8.4	40.5±2.8	±7
13.4	48.8±3.4	±7
18.4	50.0±3.5	±4
23.4	48.0±3.4	±4
28.4	44.6±3.1	±4
33.4	40.8±2.3	±4
38.4	37.2±2.1	
48.4	34.8±1.9	
73.4	28.2±1.6	
98.4[b]	23.1	
148.4	18.3±1.3	
198.4	16.6±1.4	
298.4	12.3±1.0	
398.4	10.6±0.9	
488.4	9.0±0.8	

[a] Due to the difficulty of determining $j(z)$, hence F, when the electron beam begins to flare. No other systematic effects in the relative cross section were quantitatively identified. See Sec. III F for a discussion of tests for such effects.
[b] Error in absolute cross section at this value must include a limit of systematic error of +16%, −21%, and a probable error of ±10%.

and changes in apparatus. This included a complete move of the apparatus to a new location. The agreement between these sets of data taken since the previously published results[6] for H^- is indicated by the probable errors given in Tables I and II.

F. Tests to Validate Data

A necessary but not sufficient condition that spurious or other unknown effects are not present in this experiment is that the detected signal have the functional dependence shown in Eq. (2). Examples of data showing dependences on the electron current J, the ion current I, and the form factor F at 100 eV are shown in Figs. 7–9, which are from the H^- data. Similar data exist for O^-. Correct functional dependence on the velocity of the hydrogen negative ions is demonstrated by the comparison of the signal from H^- ions with that from D^- ions of same energy (Fig. 10). With such data we prove that the signal depends on all of the variables in Eq. (2) in the required manner.

In Sec. III, three sources of possible unwanted signal were discussed and tests for their presence described. Pressure modulation of the vacuum is minimized by the use of the high electron chopping frequency and the demonstration that the same result is obtained at 20 and 5 kHz. One would also expect out-gassing to depend on the pressure history of the collision chamber.

To test for possible mixing of electron and ion modulation frequencies in the neutral detector or its associated electronics, we deliberately increase by a factor of 3 the stripped neutral signal by raising the background pressure (Fig. 11). Then, when weak or negligible (a few percent) pressure dependence of the

TABLE II. O^- detachment cross section.

Electron energy (eV)	Cross section (πa_0^2)	Limit of systematic error in relative cross section[a] (%)
7.1	5.55±0.43	7
12.1	7.00±0.40	7
17.1	8.32±0.43	4
22.1	8.69±0.43	4
27.1	8.65±0.43	
37.1	9.45±0.47	
47.1	8.95±0.45	
97.1[b]	6.30	
197.1	4.66±0.35	
297.1	3.65±0.28	
397.1	3.25±0.24	
487.1	2.90±0.22	

[a] Represents quantitative estimates that could be made. See Sec. III F for a discussion of tests for systematic errors.
[b] Error in absolute cross section at this value must include a limit of systematic error of +16%, −21%, and a probable error of ±10%.

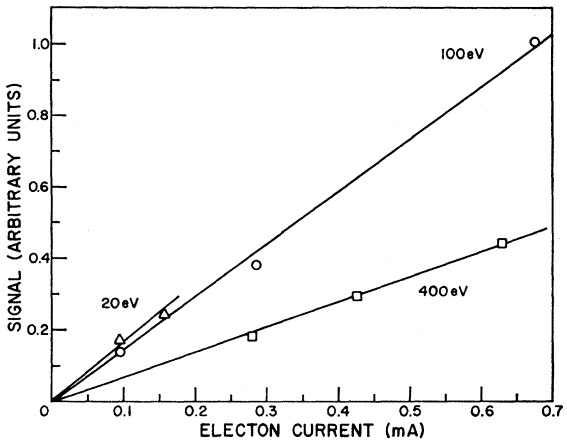

FIG. 7. Example of the dependence of the signal from H^- ions on the electron current. Highest current values for each electron energy are where data were typically taken.

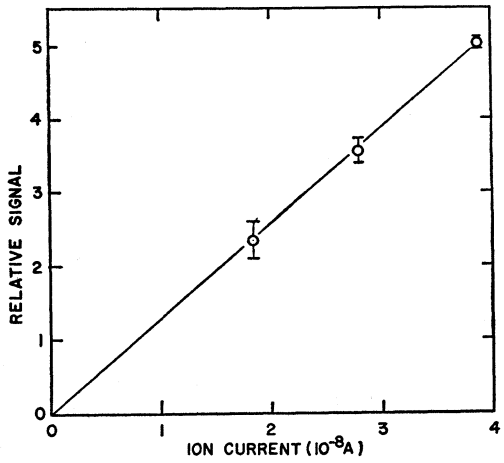

FIG. 8. Example of the dependence of the signal from H^- ions on the ion current.

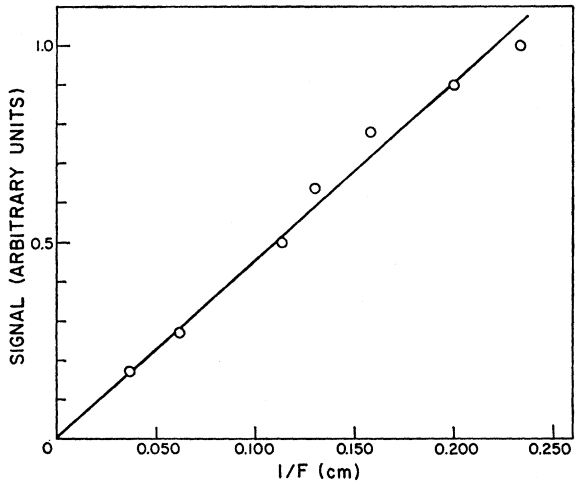

FIG. 9. Example of the dependence of the signal on the form factor F, defined in Eq. (8), for H^- with 100-eV electron energy. The form factor is changed by intersecting both beams with the scanning plate while looking at the electron-detachment signal.

signal is observed, as illustrated for one day's data with H^- in Fig. 12, we can conclude that the detector is linear under the operating conditions.

The pressure dependence of the signal is also the best test for contributions from space-charge modulation of the detector response to neutrals produced by stripping in background gas. Pressure dependences were taken at each electron energy each time measurements of the ionization cross sections were made. The different slopes in Fig. 12 are due to a combination of effects. Since the shape of the electron beam changes with electron energy, we cannot expect the same amount of spurious signal contribution over the whole electron energy range. Also, drifting of the position of the ion beam during the day can change the slope at any given energy. The slope at 100-eV electron energy, which was usually taken many times during the day,

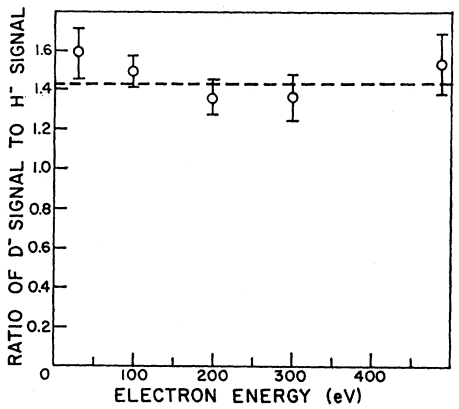

FIG. 10. Comparison of the D^- and H^- signal at different electron energies. The ratio of D^- to H^- signal should approach $\sqrt{2}$ at the energies shown here, if spurious signals due to space-charge modulation are absent.

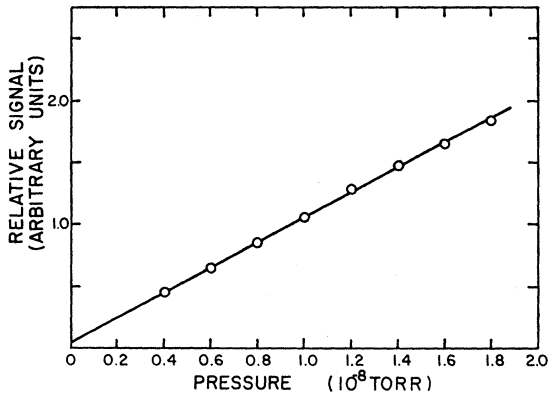

FIG. 11. Extrapolation of the background signal to zero pressure. Extrapolations such as this show that stripping of the negative ions on surfaces and slit edges contribute less than 5% to the total background signal.

was found to change due to such effects, but the intercept of the pressure dependence was reproducible.

There remains the possibility of pressure-independent neutrals modulated by the space charge. If the signal were due entirely to this cause, the ratio of D^- to H^- signals, shown in Fig. 10, would be 1.0, because in the absence of magnetic fields the two beams, having the same energy and similar cross sections for stripping, will have the same trajectory and produce the same number of neutrals. If spurious signals are entirely absent, the ratio of D^- and H^- signals is approximately[24] $\sqrt{2}$. We do not know, *a priori*, the phase that the spurious signal might have relative to the true signal. If spurious signal were present and added to the true signal, the D^-/H^- ratio should lie between 1.0 and

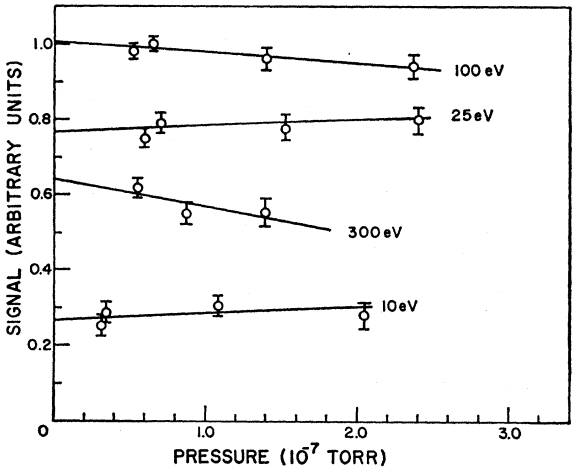

FIG. 12. Examples of the pressure dependence of the signal from one day's data. Signals are extrapolated to zero pressure by using the method of least squares to fit a straight line to the data.

[24] The center-of-mass correction requires that at 30-eV electron energy (the lowest point in Fig. 10) the ratio of the D^- to H^- signal should be 2% less than $\sqrt{2}$, which is negligible here. Strictly speaking, the dashed line in Fig. 10 should approach 1.0 at $\epsilon=0$.

$\sqrt{2}$. If we find this ratio larger than $\sqrt{2}$, we might suspect that a negative spurious signal contribution is causing an underestimate of the true cross section. If we average the points in Fig. 10, we find the ratio to be 1.45 ± 0.05, which can be shown to imply a fractional contribution independent of ion velocity (and thus presumed to be a slit-edge effect) of 0.1 ± 0.1. We would conclude that an upper bound to such effects is a 20% decrease in signal due to such effects, but no contribution to the signal is equally probable. Unfortunately, this test is not available for O^-, since it depends on the existence of two isotopes with the same electron ionization cross section.

As an alternative to the comparison of D^- and H^- signals as a test for space-charge modulation effects one can use one ion and vary the ion kinetic energy. Then one must be very careful to keep the ion-beam geometry constant. This test is used by Dance, Harrison, and Rundel,[7] who varied the H^- energy from 5 to 25 keV while holding the electron energy "at 50 eV." It is not clear, in the paper by Dance *et al.*, whether the electron gun was adjusted to keep the center-of-mass electron energy constant; if not, one must correct for the change in cross section with energy near 50 eV. However, we have subsequently been assured[17] that the electron energy was adjusted in these tests.

A more strenuous test for spurious signals is the dependence of signal on the deflection field which sweeps the ions out of the neutral beam in front of the neutral detector. The voltage across these plates should not influence the trajectories of the neutral particles created in the collision region, but might be expected to change dramatically the tiny fraction of ions which may encounter the deflector plates themselves. Figure 13 shows that over a very wide range of voltages the signal is approximately independent of voltage, even though in this range the ions move completely out of their collector cup. When the signal begins to rise very rapidly with 500 V on the plate, the ions are striking the lower plate at a location which can be seen by the entrance aperture to the neutral detector.

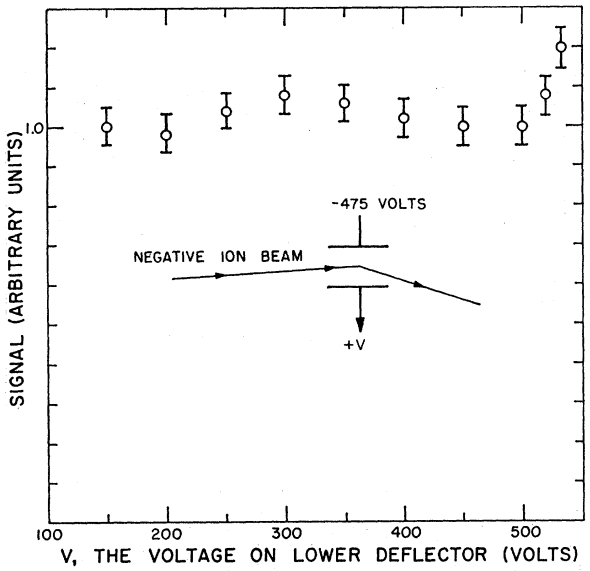

FIG. 13. Test for production of signal on the edge of the deflection plates by changing trajectory of the ions through the deflection plates. Subsequent to this test the upper plate was replaced by a wire mesh, further reducing the possibility of scattering from this plate.

Perhaps the most sensitive test of all for effects of neutral conversion on slit edges is the test illustrated in Fig. 9. Here, at 100-eV electron energy, the form factor F was deliberately varied from $F^{-1}=0.04$ to 0.23 by sweeping the scanning plate through the reaction region while the experiment was running. Thus for each value of z, specifying the position of the scanning plate, the signal and the form factor for the beams passing the plate can be measured. Clearly, when the plate is out of the beams ($z=0$), ions passing through the center of the reaction region are present along with those which pass near the edge of the entrance apertures. When the scanning plate has moved a short distance, one edge of the ion beam is cut out. When it passes the center of the beams, the part of the ion current which certainly does not graze the entrance slit is being removed. Finally, the opposite edge of the ion beam is examined just before the plate extinguishes the signal. If slit-edge conversion of neutrals were a significant contributor to the signal, the edges of the ion beam would certainly provide a larger part of it than the center of the beam. There is no evidence for such an affect. Of course, the scanning plate itself will influence the space charge, but in the present geometry this will not be a large effect.

V. RESULTS AND CONCLUSIONS

The results of our experimental measurements are given in Tables I and II along with the random and systematic error estimates. These results are compared with Bethe-Born calculations in Figs. 14 and 15.

The error bars shown in Fig. 14 for H^- represent 50% confidence limits in the cross section relative to the cross section at 100 eV (corrected electron energy). The 50% confidence limits for the O^- cross section relative to 100 eV are the same order of magnitude as the circles representing the data, and hence are not shown on the graph. The uncertainty in the cross sections shown in the center columns of Tables I and II represent 50% confidence limits in the cross section *relative* to the cross section at 100 eV. These uncertainties are obtained by averaging data at each electron energy from complete cross-section measurements made on different occasions, each normalized at 100 eV. They demonstrate the good reproducibility in shape of the cross section, because the statistical error in a single measurement at one energy is typically from 2 to 10%. Seven sets of O^- data and five sets of H^- data were combined.

The 50% confidence limits in the random error and the estimated limit of systematic effects for the *absolute* cross section at 100 eV are also given in the tables. The limit of systematic effects includes calibration of the neutral detector (4%), measurement of the ion-beam current (5%), measurement of the electron current (2%), and the uncertainty in the calculation of the form factor [−5% with an additional ±5% for the form factor due to possible variations $i(z)$ in the direction of the electron beam]. These estimates were linearly combined to give a limit for the systematic errors in the cross section at 100 eV. The uncertainty in the relative cross section at the lower electron energies is due to the effect of the divergence of the electron beam on the form factor F, for if the electron beam is diverging, F is properly written as

$$IJF=\int_V i'(y,z)j'(y,z)dy\,dz\,, \tag{19}$$

where y is the direction of the electron beam. The limit of any systematic effect is determined by calculating what the difference in signal would be if the ion beam were entirely at either side of the limiting aperture, a very conservative assumption.

The theoretical calculation of the H^- cross section shown in Fig. 14 is that of McDowell and Williamson[2] which also includes the semiclassical Coulomb correction of Geltman. The theoretical calculation has not included the possibility of leaving the H^0 atom in an excited state. The contribution to the photodetachment cross section for an atom left in the $n=2$ state has been calculated and was found to be a large (17%) contribution to the total oscillator strength.[25]

The O^- data are compared with the Bethe-Born approximation. The cross section for electron detachment is given in terms of the photodetachment cross section $\sigma_{\rm ph}(\epsilon)$ by

$$\sigma_{\rm det}(E)=\frac{R}{\pi\alpha E}\int_0^{(1/2)(E-I)}\frac{\sigma_{\rm ph}(\epsilon)}{I+\epsilon}\ln\frac{4E}{I+\epsilon}d\epsilon\,, \tag{20}$$

where E is the electron energy, α is the fine-structure constant, I is the electron affinity, ϵ is the ejected electron energy above threshold, and R is rydberg. The photodetachment cross section used in this calculation was a combination of experimental[22] and theoretical[26] data. The calculation of the O^- electron detachment includes the contributions to the photodetachment cross section that occur when the O atom is left in the ^1D and ^1S metastable states. Recent calculations[27] of the O^- photodetachment cross sections indicate that the photodetachment cross section at the energies above the ^1D threshold might not be as large as previous calculations have indicated. However, our calculation makes allowance for the channels leading to electronic excitation of the oxygen atom at higher energies. The Coulomb correction of Geltman was then applied to the resulting cross section. Here it should be noted that this semiclassical correction is particularly questionable at the lower energies for O^- since the impact parameter is approaching the size of the electron wavelength. From this comparison we can conclude that the Bethe-Born approximation with the semiclassical correction predicts the magnitude of the electron-detachment cross section very well in the region of 20 to 50 eV, but does not give meaningful results below this.

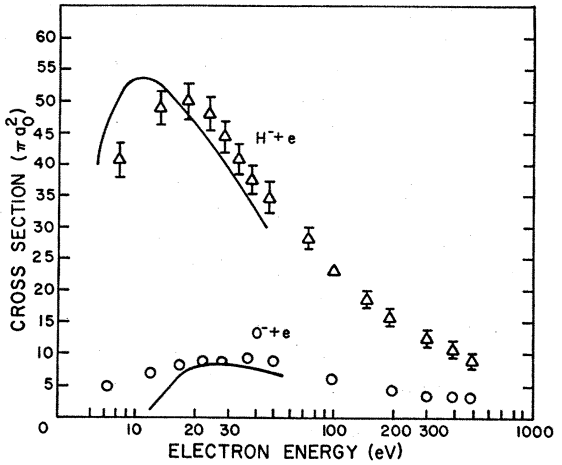

FIG. 14. Comparison of our experiment for H^- and O^- results with Bethe-Born approximations which include a semiclassical Coulomb correction.

It is interesting to note that the maxima for the H^- and O^- cross sections come at about 18 and 37 eV, respectively, which is quite accurate in the ratio

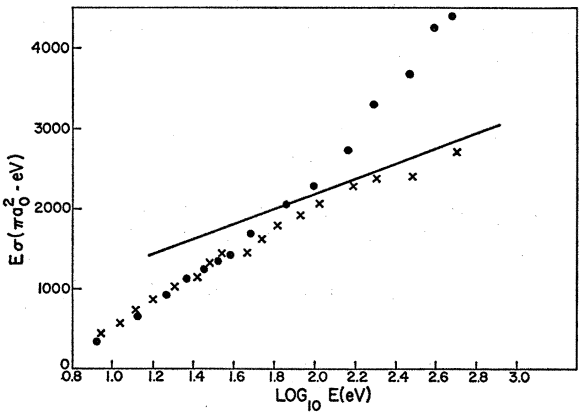

FIG. 15. The Born approximation predicts that the H^- ionization cross section should approach asymptotically at high energy an energy dependence which would give a straight line on this plot, with a slope given by the solid line in the figure. The slope is calculated in Sec. V, and the solid line is located on the diagram consistent with the theory of Inokuti and Kim (Ref. 31). The black dots are data of this paper, the crosses those of Dance, Harrison, and Rundel (Ref. 7).

[25] J. Macek, Proc. Phy. Soc. (London) **92**, 365 (1967).
[26] J. W. Cooper and J. B. Martin, Phys. Rev. **126**, 1482 (1962).
[27] R. J. W. Henry, Phys. Rev. **162**, 56 (1967).

of the electron affinities, as expected classically. But the maximum values for the cross sections ($50\pi a_0^2$ and $9.5\pi a_0^2$, respectively), while well predicted with the impact-parameter modified Bethe-Born theory, are in the ratio 5.2, and not 0.63 as would be predicted from the Thomson theory.[28]

At low energies there are as yet no calculations of the H^- or O^- cross sections which are sufficiently free of semiempirical treatment to provide a truly independent test of theory or to give confidence in the theoretical predictions for the energy region below 8 eV. However, in the limit of high electron energies the Born approximation predicts that the energy dependence of the cross section is described with increasing accuracy by

$$E\sigma(E)=A\ \ln E+B, \tag{21}$$

where A and B are constants. Equation (20) reduces to this form at energies sufficiently high that the integrand has become negligible at the upper limit of the integral, and when terms of the order E^{-1} are small compared to those of order $E^{-1}\ln E$:

$$\sigma_{\rm det}\rightarrow\frac{1}{\pi\alpha}\left\{\int_0^\infty\sigma_{\rm ph}\frac{d\lambda}{\lambda}\right\}\frac{\ln E/R}{E/R}. \tag{22}$$

The integral in brackets can be performed using computed photodetachment cross sections, but it is more convenient to appeal to a sum rule,[29,31,38] which will have the virtue that it will include the effects of photodetachment into all possible final states just as the experiment does. This sum rule can be written

$$\sum_n\frac{Rf_{\rm on}}{E_n-E_0}+\int_0^\infty\frac{df}{d\epsilon}\frac{d\epsilon}{(\epsilon/R)}=\frac{1}{3a_0^2}\langle(\sum\bar{r}_i)^2\rangle_{00}, \tag{23}$$

where f_{0n} is the oscillator strength of the discrete transition from the ground state to the state n, and $df(\epsilon)/d\epsilon$ is related to the photodetachment cross section by the relation

$$\frac{df(\epsilon)}{d\epsilon}=\frac{1}{2\pi^2\alpha a_0e^2}\sigma_{\rm ph}(\epsilon). \tag{24}$$

From Pekeris[30] we find $\frac{1}{3}\langle(\sum\bar{r}_i)^2\rangle_{00}=7.484$ for H^-, and the first term in Eq. (23) is zero since there is only one bound state. Thus by combining Eqs. (24) and (23) in (22) we find, with σ in units of πa_0^2 and E in eV,

$$\frac{d(\sigma_{\rm ion}E)}{d(\log_{10}E)}=940. \tag{25}$$

This method of obtaining the slope of the cross-section curve is the same as that developed earlier by Inokuti and Kim[31] and recently brought to our attention. They are also able to calculate B and obtain an absolute cross section.

In Fig. 15 we see a plot of $E_{\rm ion}$ against $\log_{10}E$, giving both our data (black dots) and the data of Dance *et al.*[7] The theoretical limiting slope of 940 is drawn in as a black line. The absolute magnitude is consistent with that found by Inokuti and Kim.[31] It is noted that our data are not consistent with such a low slope, for at energies from 100 to 500 eV, these data give a slope of about 2500, and from 11 eV to 155 eV a slope of about 1900.

The tests we have made for systematic errors which might explain the difference between our data and that of DHR are described in the previous section. The test shown in Fig. 10 should reveal pressure-independent effects of space-charge modulation. The energy dependence of the D^-/H^- signal ratio, as shown in Fig. 10, is of the wrong slope from 200 to 500 V to explain the discrepancy with DHR. If we assume that their cross section at 500 eV is correct and ours is in error due to a positive contribution from ions modulated by the electron space charge and stripped on a metal surface, the D^-/H^- ratio at 500 eV should have been 1.28 instead of 1.51 ± 0.15 as observed, and 1.414 as expected for pure ionization-cross-section signal.

Dance, Harrison, and Rundel compare their data with the Bethe approximation limiting slope only after dividing the data by the classical trajectory correction given by Geltman. This is not consistant with the Coulomb correction that is used by McDowell and Williamson[32] for the theoretical cross section presented in the paper by Dance *et al.* This theory uses a Coulomb correction of the form

$$Q_C=Q_{BB}(1-2/E\sqrt{Q_{BB}}),$$

where Q_{BB} is in πa_0^2. Geltman's correction is of the form

$$Q_C=Q_{BB}[1-(2\sqrt{\pi})/E\sqrt{Q_{BB}}].$$

Because of the questionable validity of this correction, this appears to us not to be a useful comparison, and we have not made such a correction in Fig. 15. If we draw a best straight line through their points in the same manner as done by DHR, i.e., fitting the data from 20 to 200 eV, we find a slope of 1340. We can then make the following conclusions:

(1) Our data and those of DHR do not give the same slope when σE is plotted against $\log_{10}E$ at energies above about 100 eV.

(2) If one wishes to insist that the data be linear in such a plot for all energies above the maximum in the cross section, as is stated in the paper by DHR, then *both* our data and the data of DHR give larger slopes than the sum rule (940).

[28] J. J. Thomson, Phil. Mag. **23**, 419 (1912).
[29] W. F. Miller and R. L. Platzman, Proc. Phys. Soc. (London) **A70**, 299 (1957).
[30] C. L. Pekeris, Phys. Rev. **126**, 1470 (1962).
[31] M. Inokuti and Y.-K. Kim, Bull. Am. Phys. Soc. **13**, 38 (1968); Phys. Rev. (to be published).
[32] M. R. C. McDowell (private communication).

(3) If one does not insist on this, but considers the slope of the data of DHR from about 100 to 500 eV only, they are consistent with the sum rule.

(4) On experimental grounds *alone*, we are not able to account for sufficiently large systematic errors in our relative cross section to give the differences observed. The quoted random errors in the two experiments are irrelevant to the discussion of this systematic difference, since in each experiment the data points are seen to fall in relatively smooth curves.

(5) The comparison discussed by Wareing and Dolder[10] is misleading. They have compared cross sections for ionization of Li^+, He, and H^-, which are isoelectronic, expecting the cross sections to scale classically in the following manner:

$$I^2\sigma_{\text{ion}}=S(E/I)^{-1}\ln(E/I)\pi a_0^2, \tag{26}$$

where I is the ionization potential of the target atom, and S is presumed a constant of proportionality independent of electronic structure. But Geltman[33] has used the sum rule of Eq. (23) to compute S for these three two-electron atoms:

$$S=4RI\left\{\frac{1}{3a_0^2}\langle(\sum\bar{r}_i)^2\rangle_{00}-\sum_n\frac{Rf_{\text{on}}}{E_n-E_0}\right\}. \tag{27}$$

For He, Geltman took the first term in curly brackets in Eq. (27) to be 0.7525 from Pekeris,[34] and the oscillator strength sums from Trefftz *et al.*[35] tabulated by Stewart.[36] The result $S_{\text{He}}=680$ is obtained. This can be compared with $S_{H^-}=308$ in the same units. The same result is found from the direct numerical iteration of $\int(df/d\epsilon)(d\epsilon/\epsilon)$ using $df/d\epsilon$ calculated by Stewart and Webb.[37] Their results were obtained with Hartree-Fock wave functions in the dipole length approximation. The asymptotic slope for H^- can be compared with the slope for He which has also been calculated in a recent paper by Inokuti *et al.*[38]

For Li^+, Geltman integrated Stewart and Webb's calculated continuum oscillator strengths to find $S_{Li^+}=631$. Thus, it is found that the negative ion is indeed not typical of the hydrogenic members of the isoelectronic sequence, and when $I^2\sigma$ is plotted against $(E/I)^{-1}\ln(E/I)$, as is done in the paper of Wareing and Dolder, one expects the slope of the H^- curve to be less than half of the curves for He and Li^+, while the latter lie within about 10% of one another.

It is unfortunate that a similar comparison is not available for the O^- data, but the requisite expectation value for $(\sum\bar{r}_i)^2$ in the ground state has not to our knowledge been computed.

ACKNOWLEDGMENTS

The authors would like to thank S. Geltman of the Joint Institute for Laboratory Astrophysics for the computations for the last section, as well as for his continued interest in this problem over a number of years. Gordon Dunn has provided useful criticisms of our work. We are grateful to D. F. Dance, M. F. A. Harrison, and R. D. Rundel for communication of their results prior to publication, and to Mitio Inokuti and Yong-Ki Kim of the Argonne National Laboratory for communicating their work on the H^- sum rule. John Hall of the Joint Institute for Laboratory Astrophysics suggested the double-modulation scheme and Stephen J. Smith called to our attention the dependence on pumping speed, volume, and modulation frequency of the amplitude of the background pressure modulations due to the electron beam.

[33] S. Geltman (private communication).
[34] C. L. Pekeris, Phys. Rev. **115**, 1216 (1959).
[35] E. Trefftz, A. Schlüter, Ki-Hi Dettmar, and K. Jörgens, Z. Astrophysik **44**, 1 (1957).
[36] A. L. Stewart, Advan. Phys. **12**, 299 (1963).
[37] A. L. Stewart and T. G. Webb, Proc. Phys. Soc. (London) **82**, 532 (1963).
[38] M. Inokuti, Y.-K. Kim, and R. L. Platzman, Phys. Rev. **164**, 55 (1967).